



# Synthesis and electrical properties of novel oligomer semiconductors for organic field-effect transistors (OFETs): Asymmetrically end-capped acene-heteroacene conjugated oligomers



Jang Yeol Back <sup>a,1</sup>, Yebyeol Kim <sup>b,1</sup>, Tae Kyu An <sup>b</sup>, Moon Seong Kang <sup>c</sup>, Soon-Ki Kwon <sup>a,\*\*\*</sup>, Chan Eon Park <sup>b,\*</sup>, Yun-Hi Kim <sup>c,\*\*</sup>

<sup>a</sup> School of Materials Science and Engineering and Research Institute for Green Energy Convergence Technology (REGET), Gyeongsang National University, Jin-ju 660-701, Republic of Korea

<sup>b</sup> POSTECH Organic Electronics Laboratory, Polymer Research Institute, Department of Chemical Engineering, Pohang University of Science and Technology, Pohang 790-784, Republic of Korea

<sup>c</sup> Department of Chemistry and ERI, Gyeongsang National University, Jin-ju 660-701, Republic of Korea

## ARTICLE INFO

### Article history:

Received 25 April 2014

Received in revised form

7 July 2014

Accepted 10 July 2014

Available online 18 July 2014

### Keywords:

Organic field-effect transistor  
Small molecule semiconductor  
Solubility  
Conjugated core modification  
End-group

## ABSTRACT

Noble small molecules composed of an aromatic phenylene-trithiophene and naphthalene-trithiophene conjugated core were synthesized and examined for their property in p-type OFET devices. The phenylene and naphthalene moieties were combined with a trithiophene to introduce torsional structures into the conjugated core and improve the solubility compared with the solubility of the quaterthiophene core containing molecule. Although phenylene-trithiophene and naphthalene-trithiophene containing molecules showed lower mobilities ( $2.9 \times 10^{-3}$  and  $1.04 \times 10^{-2}$  cm<sup>2</sup>/V, respectively) than quaterthiophene containing molecule ( $3.21 \times 10^{-2}$  cm<sup>2</sup>/V), they showed more film uniformity caused by improved solubility. The thermal stability, photochemical properties, and morphological characteristics were investigated using TGA, DSC, cyclic voltammetry, and XRD techniques.

© 2014 Elsevier Ltd. All rights reserved.

## 1. Introduction

Solution-deposited organic semiconductors have been widely studied due to their suitability for large-area processing, their mechanical flexibility, and their light weight [1–10]. Small molecule semiconductors are particularly profitable for electronic applications because they can be reliably synthesized with accurate molecular weight control without significant batch-to-batch variations [11,12]. Additionally, small molecule semiconductors can potentially provide high-quality chain alignment.

Electronic applications require that small molecule semiconductors satisfy several criteria, in addition to providing good electrical properties: i) they must form a thin film with a well-

developed morphology that includes short  $\pi$ – $\pi$  distances, favorable chain conformations, and submicron-sized crystal structures without defects [7,11,13–15]; and ii) the molecular structure must provide an appropriate highest occupied molecular orbital (HOMO), lowest unoccupied molecular orbital (LUMO), and must yield devices that provide stable operation and resist oxidation over time [16,17].

The components of small molecules, including the end groups, conjugated core, and substituted heteroatoms, may be modified through systematic investigations in an attempt to optimize the molecular structures [18]. Above all, modifications to the conjugated core provide a key method for controlling the electrical properties of the organic semiconductor, such as the electron affinity, ionization potential, inter/intramolecular interactions, and solubility in organic solvents. Previous work in our group has investigated the quaterthiophene conjugated core with bulky end groups, which displayed adequate field-effect mobility [19,20]; however, the quaterthiophene core did not convey sufficient solubility to provide uniform film morphology during solution-processing as the organic semiconductor.

\* Corresponding author.

\*\* Corresponding author.

\*\*\* Corresponding author.

E-mail addresses: [skwon@gnu.ac.kr](mailto:skwon@gnu.ac.kr) (S.-K. Kwon), [cep@postech.ac.kr](mailto:cep@postech.ac.kr) (C.E. Park), [ykim@gnu.ac.kr](mailto:ykim@gnu.ac.kr) (Y.-H. Kim).

<sup>1</sup> Jang Yeol Back and Yebyeol Kim contributed equally.

This study sought to enhance the solubility of the small molecule semiconductors by combining phenylene and naphthalene aromatic rings into the tri-thiophene conjugated core, which offer a rigid torsional structure due to topological constraints [21] to yield a homogeneous thin film. The phenylene-modified cyclohexylethynyltrithiophenophenylene (CHE3TP) and naphthalene-modified cyclohexylethynyltrithiophenenaphthalene (CHE3TN) were synthesized and characterized as semiconductors for use in OFETs. The electron-rich triple bond in CHE3TP and CHE3TN extended the  $\pi$ -system of the conjugated core and improved the molecular rigidity [22].

CHE3TP and CHE3TN compounds were characterized by thermogravimetric analysis (TGA), differential scanning calorimetry (DSC), UV–vis spectroscopy, and X-ray diffraction (XRD) techniques. Density functional theory (DFT) calculations were performed to investigate their electronic structures.

## 2. Experimental

### 2.1. Materials and synthesis

#### 2.1.1. Materials

2-Bromothiophene, *N*-bromosuccinimide (NBS), *n*-butyllithium, 2-isopropoxy-3,3,4,4-tetramethyl-1,3,2-dioxaborolane, 1,3-bis(diphenylphosphinopropane)-dichloronickel, *N,N*-dimethylformamide (DMF), copper(I), sodium carbonate, 2,2-bipyridine, 1,5-cyclooctadiene, bis(cyclooctadiene)nickel(0), dichloro-((bis(diphenylphosphino)ferrocenyl)palladium(II), cyclohexylacetylene, and tetrakis(triphenylphosphine)palladium(0) were purchased from Aldrich.

#### 2.1.2. Synthesis of 2-(cyclohexylethynyl)thiophene (1)

CuI (1.07 g, 5.62 mmol) and Pd(dppf)Cl<sub>2</sub> (0.75 g, 0.93 mmol) were added to a mixture of 2-bromothiophene (10 g, 98.30 mmol) and di(isopropylamine) (200 mL), followed by heating at 50 °C. After the slow addition of cyclohexylacetylene (15.29 g, 93.80 mmol) to the mixture, the reaction mixture was stirred for 4 h at 80 °C. The crude product was extracted with ethyl acetate (3 × 200 mL) and the combined extracts were dried over anhydrous magnesium sulfate and purified by column chromatography using hexane as the eluent. Yield: 16.5 g (92%); IR (KBr, cm<sup>-1</sup>): 2221 (alkyne), <sup>1</sup>H NMR (CDCl<sub>3</sub>, 300 MHz, ppm):  $\delta$  = 7.15 (dd, *J* = 5.2 Hz, 1H), 7.10 (dd, *J* = 3.7 Hz, 1H), 6.92 (dd, *J* = 5.2 Hz, 1H), 2.42–2.41 (m, 1H), 1.90–1.86 (m, 5H), 1.46–1.23 (m, 5H).

#### 2.1.3. Synthesis of 2-(5-(cyclohexylethynyl)thiophen-2-yl)-4,4,5,5-tetramethyl-1,3,2-dioxaborolane (2) [23]

2.5 M *n*-BuLi (32.8 mL, 95.63 mmol) was added to a mixture of 2-(cyclohexylethynyl)thiophene (13 g, 68.31 mmol) and tetrahydrofuran (THF) (250 mL) at –78 °C. After stirring for 1 h, 2-isopropoxy-4,4,5,5-tetramethyl-1,3,2-dioxaborolane (17.8 g, 81.97 mmol) were added. After stirring for 12 h, the crude product was extracted with ethyl acetate (3 × 200 mL) and water (200 mL). The pure product was obtained by column chromatography using hexane as the eluent. Yield: 4 g (25%); IR (KBr, cm<sup>-1</sup>): 2215 (alkyne), 2847–2973 (aliphatic CH<sub>3</sub>), <sup>1</sup>H NMR (CDCl<sub>3</sub>, 300 MHz, ppm):  $\delta$  = 7.46–7.45 (d, *J* = 3 Hz, 1H), 7.16–7.15 (d, *J* = 3 Hz, 1H), 2.65–2.59 (m, 1H), 1.95–1.73 (m, 5H), 1.60–1.41 (m, 5H), 1.34 (s, 12H).

#### 2.1.4. Synthesis of 5-bromo-5'-phenyl-2,2'-bithiophene (3)

A mixture of 5,5'-dibromo-2,2'-bithiophene (5 g, 15.42 mmol) and phenylboronic acid (5 g, 12.34 mmol) were added to a mixture toluene (50 mL), 2 M K<sub>2</sub>CO<sub>3</sub> (10 mL), and tetrakis(triphenylphosphine) palladium(0) (0.17 g, 1.47 × 10<sup>-4</sup> mol). After stirring for 48 h at 85 °C, 2 N HCl (40 mL) was added. The crude

product was extracted with dichloromethane and purified by column chromatography using hexane as the eluent. Yield: 2.3 g (60%); IR (KBr, cm<sup>-1</sup>): 3031–3064 (aromatic CH), <sup>1</sup>H NMR (300 MHz, CDCl<sub>3</sub>, ppm):  $\delta$  = 7.62–7.59 (m, *J* = 5.2 Hz, 2H), 7.40–7.38 (t, *J* = 3.9 Hz, 2H), 7.31–7.28 (m, 1H), 7.24–7.23 (d, *J* = 3 Hz, 1H), 7.10–7.09 (d, *J* = 3 Hz, 1H), 7.01–6.95 (dd, *J* = 9 Hz, 2H).

#### 2.1.5. Synthesis of 5-bromo-5'-(naphthalen-2-yl)-2,2'-bithiophene (4)

A mixture of 5,5'-dibromo-2,2'-bithiophene (6 g, 18.51 mmol) and naphthalene-2-ylboronic acid (2.22 g, 12.95 mmol) were added to toluene (80 mL), 2 M K<sub>2</sub>CO<sub>3</sub> (15 mL), and tetrakis(triphenylphosphine) palladium(0) (0.17 g, 1.47 × 10<sup>-4</sup> mol). After stirring for 48 h at 85 °C, 2 N HCl (40 mL) were added. The crude product was extracted with dichloromethane and purified by column chromatography using hexane as the eluent. Yield: 2.5 g (53%); IR (KBr, cm<sup>-1</sup>): 3031–3064 (aromatic CH), <sup>1</sup>H NMR (300 MHz, CDCl<sub>3</sub>, ppm):  $\delta$  = 8.04 (s, 1H), 7.88–7.86 (m, 3H), 7.76–7.75 (d, *J* = 1.8 Hz, 1H), 7.52–7.48 (m, 2H), 7.37–7.35 (d, *J* = 3.9 Hz, 1H), 7.15–7.14 (d, *J* = 3.6 Hz, 1H), 7.02–6.98 (m, 2H).

#### 2.1.6. Synthesis of 5-cyclohexylethynyl-5'-phenyl-[2,2',5',2'] quaterthiophene (CHE3TP)

2-(5-(Cyclohexylethynyl)thiophen-2-yl)-4,4,5,5-tetramethyl-1,3,2-dioxaborolane (1.77 g, 5.6 mmol) and 5-bromo-5'-phenyl-2,2'-bithiophene (1.8 g, 5.6 mmol) were added to toluene (50 mL), 2 M K<sub>2</sub>CO<sub>3</sub> (10 mL), THF (8 mL), and tetrakis(triphenylphosphine) palladium(0) (0.05 g, 0.43 × 10<sup>-4</sup> mol). The reaction mixture was stirred for 48 h at 85 °C, and 2 N HCl (400 mL) were added at room temperature. The crude product was extracted with dichloromethane (3 × 300 mL) and purified by column chromatography using hexane as the eluent. Yield: 1.1 g (46%); mp = 191 °C, IR (KBr, cm<sup>-1</sup>): 3050 (aromatic C–H), 2215 (alkyne), and 2847–2973 (aliphatic C–H) <sup>1</sup>H NMR (300 MHz, CDCl<sub>3</sub>, ppm):  $\delta$  = 7.63–7.60 (t, *J* = 7.2 Hz, 2H), 7.43–7.38 (t, *J* = 7.2 Hz, 2H), 7.30–7.24 (m, 2H), 7.17–7.15 (d, *J* = 7.2 Hz, 1H), 7.11–7.07 (m, 2H), 7.03–7.00 (m, 2H), 2.66–2.60 (m, 1H), 1.92–1.75 (m, 5H), 1.53–1.27 (m, 5H). HR-MS Found 430.0891, requires 430.0884.

#### 2.1.7. Synthesis of 5-cyclohexylethynyl-5'-naphthalene-2-yl-[2,2',5',2']terthiophene (CHE3TN)

2-(5-(Cyclohexylethynyl)thiophen-2-yl)-4,4,5,5-tetramethyl-1,3,2-dioxaborolane (1.7 g, 4.57 mmol) and 5-bromo-5'-(naphthalene-2-yl)-2,2'-bithiophene (1.54 g, 4.57 mmol) were added to toluene (50 mL), 2 M K<sub>2</sub>CO<sub>3</sub> (10 mL), THF (8 mL) and tetrakis(triphenylphosphine) palladium(0) (0.05 g, 0.43 × 10<sup>-4</sup> mol). The reaction mixture was stirred for 48 h at 85 °C, and 2 N HCl (400 mL) were added at room temperature. The crude product was extracted with dichloromethane (3 × 300 mL) and purified by column chromatography using hexane as the eluent. Yield: 1.05 g (48%); mp = 220 °C, <sup>1</sup>H NMR (300 MHz, CDCl<sub>3</sub>, ppm):  $\delta$  = 8.05 (s, 1H), 7.88–7.83 (t, *J* = 6.3 Hz, 3H), 7.77–7.56 (d, *J* = 3.6 Hz, 1H), 7.52–7.47 (m, 2H), 7.39–7.37 (d, *J* = 3.9 Hz, 1H), 7.21–7.20 (d, *J* = 3.9 Hz, 1H), 7.14–7.08 (dd, *J* = 3.9 Hz, 2H), 7.04–7.03 (d, *J* = 3.9 Hz, 2H), 2.65–2.62 (m, 1H), 1.92–1.75 (m, 5H), 1.53–1.27 (m, 5H). IR (KBr, cm<sup>-1</sup>): 3063 (aromatic C–H), 2215 (alkyne), 2847–2973 (aliphatic C–H). HR-MS Found 480.1046, requires 480.1040.

### 2.2. Measurements

The <sup>1</sup>H NMR spectra were recorded using a Bruker AM-300 spectrometer. The FT-IR spectra were measured on a Bomem Michelson series FT-IR spectrometer. The thermal analysis was performed using a TA TGA 2100 thermogravimetric analyzer under

a nitrogen atmosphere with a heating rate of 20 °C/min. Differential scanning calorimetry (DSC) measurements were conducted under nitrogen using a TA instrument 2100 DSC. The samples were heated with a rate of 20 °C/min from 30 °C to 250 °C. UV–vis absorption spectra were measured using a Perkin Elmer LAMBDA-900 UV/VIS/IR spectrophotometer. UV–vis absorption studies were carried out using Perkin–Elmer LAMBDA-900 UV/VIS/IR spectrophotometer. Cyclic voltammetry (CV) was performed on an EG and G Parc model 273 Å potentiostat/galvanostat system with a three-electrode cell in a solution of  $\text{Bu}_4\text{NClO}_4$  (0.1 M) in acetonitrile at a scan rate of 100  $\text{mV s}^{-1}$ . CHE3TP and CHE3TN films were coated onto a square Pt electrode ( $0.50 \text{ cm}^2$ ) by dipping into xylene solutions containing each of the molecules and then drying in air. A Pt wire was used as the counter electrode, and an  $\text{Ag}/\text{AgNO}_3$  (0.1 M) electrode was used as the reference electrode.

Microstructural characterization of the CHE3TP and CHE3TN thin films was confirmed using XRD (beam energy: 8 keV). The samples were prepared by spin-coating a xylene solution onto the octyltrichlorosilane (OTS)-chemisorbed  $\text{SiO}_2/\text{Si}$  wafer (film thickness: 50 nm), and measurements were conducted in a vacuum chamber.

### 2.3. Fabrication and characterization of OFETs

The electrical properties of the CHE3TP and CHE3TN films were investigated using a top-contact bottom-gated OFET configuration, with a 3000 Å thick  $\text{SiO}_2$  dielectric on a heavily N-type doped silicon substrate as the gate electrode. The substrate was cleaned in piranha solution, composed of concentrated  $\text{H}_2\text{SO}_4$  (60 mL) and  $\text{H}_2\text{O}_2$  (40 mL), and modified by OTS to reduce the number of hydroxyl groups present on the  $\text{SiO}_2$  surface. The organic semiconductor thin films were formed by spin-coating at 2000 rpm from a 0.6 wt% xylene solution to a nominal thickness of 50 nm, as confirmed using an ellipsometer (J.A.WOLLAM Co., Inc.). After depositing the semiconductor film, gold source/drain electrodes were deposited (100 nm) with width-to-length ratios ( $W/L$ ) = 1000  $\mu\text{m}/100 \mu\text{m}$ . The OFET measurements were carried out in a dark room and ambient environment using Keithley 2400 and 236 source/measure units. The OFET parameters, such as the field-effect mobilities, threshold voltage, and on-off ratio, were extracted in the saturation regime ( $I_D$ : drain current =  $-80 \text{ V}$ ) using the square root of the drain current–gate voltage ( $I_D^{1/2} - V_G$ ), plotted according to the following formula:  $I_D = \mu C_{\text{diel}} (W/2L) (V_G - V_{\text{th}})^2$ , where  $\mu$  is the field-effect carrier mobility,  $C_{\text{diel}}$  is the capacitance per unit area of the dielectric layer,  $V_G$  is the gate voltage, and  $V_{\text{th}}$  is the threshold voltage [24].

## 3. Results and discussion

### 3.1. Synthesis and characterization

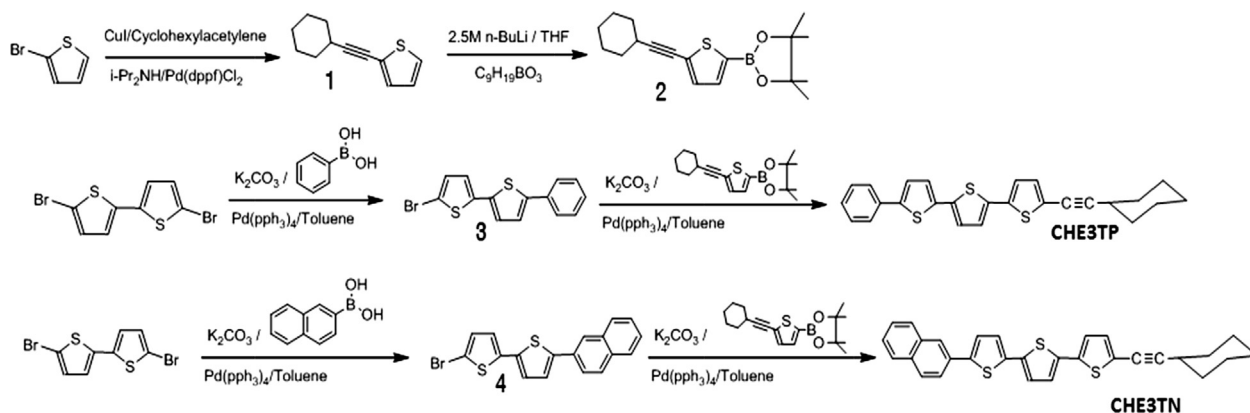
The synthetic scheme for preparing CHE3TP and CHE3TN is outlined in Scheme 1. CHE3TP and CHE3TN were synthesized by a Sonogashira and Suzuki coupling reaction. CHE3TP and CHE3TN were characterized by  $^1\text{H NMR}$ , IR, and Mass spectroscopies. CHE3TN was more soluble than CHE3TP in xylene, although both small molecules showed better solubilities than cyclohexylethynylquaterthiophene (CHE4T; the molecular structure is shown in Fig. 4).

As shown in Fig. 1, the thermal properties of the synthesized CHE3TP and CHE3TN were evaluated by TGA and DSC. The TGA measurements were conducted to investigate the device longevity [25,26]. CHE3TP and CHE3TN showed good thermal stability for use in organic electronics (5% decomposition after heating at 365 °C or 415 °C, respectively). The DSC measurements revealed that CHE3TN displayed a higher melting point (222 °C) than CHE3TP (192 °C), indicating the presence of stronger intermolecular interactions in the crystal structure of CHE3TN [27,28].

### 3.2. Photochemical properties

Fig. 2 shows the photochemical absorption spectra as measured in the UV–vis region in the solution and thin film states. CHE3TP and CHE3TN revealed absorption maxima in a dilute chloroform solution at 402 and 408 nm, respectively. The edges of the absorption peaks in the film state in both semiconductors were red-shifted relative to the peaks obtained in the solution state.

The HOMO levels of CHE3TP and CHE3TN were calculated from the oxidation onset measured using cyclic voltammetry (CV) and were shown to be 5.43 eV and 5.55 eV for CHE3TP and CHE3TN, respectively. The optical band gaps of CHE3TP and CHE3TN were extracted from the band edge obtained in the thin film state. All photochemical properties are summarized in Table 1. Computational simulations were carried out to better understand the electronic and geometric structures, as shown in Fig. 3. The HOMO and LUMO levels of CHE3TN were slightly lower than those of CHE3TP, and these results corresponded to the photochemical measurements. In both molecules, the phenylene and naphthalene moieties, which were combined with three thiophene conjugated cores, contributed less to the  $\pi$ -orbital delocalization of the HOMO and LUMO levels (Fig. 3) than the thiophene moiety in the quaterthiophene core (Fig. 4), although the tilted structure enhanced the solubility of the CHE3TP and CHE3TN molecules.



Scheme 1. Synthetic routes of the CHE3TP and CHE3TN.

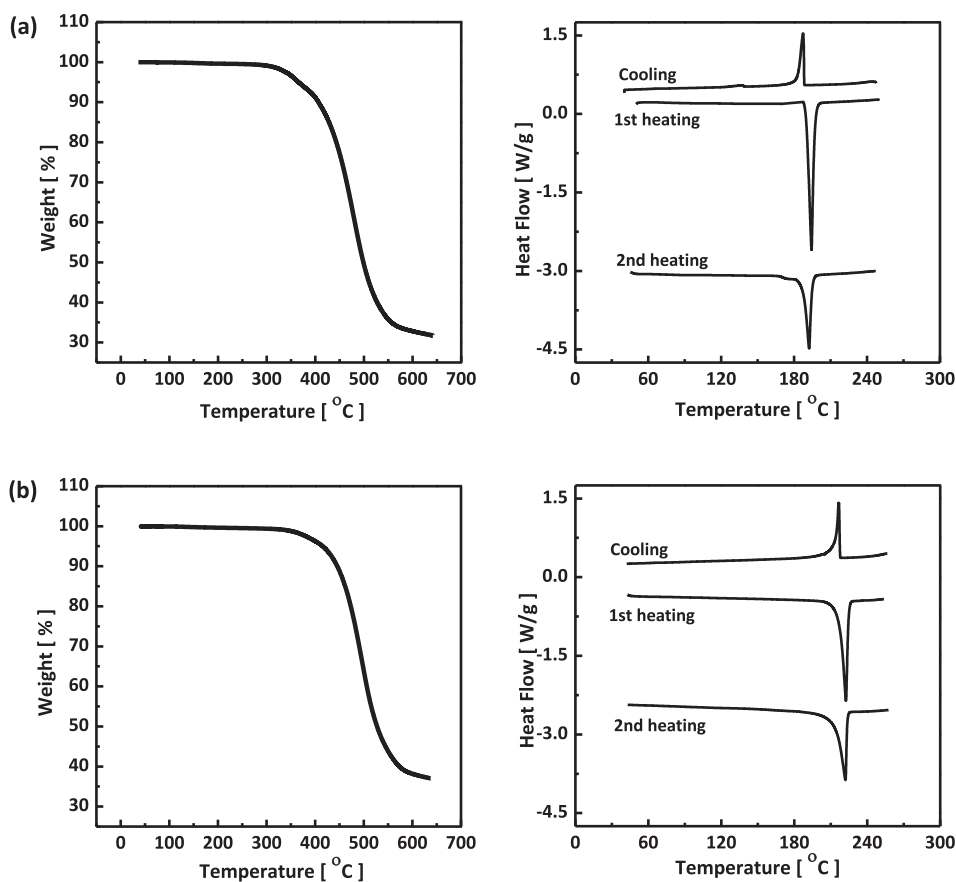


Fig. 1. DSC and TGA thermograms of CHE3TP (a) and CHE3TN (b).

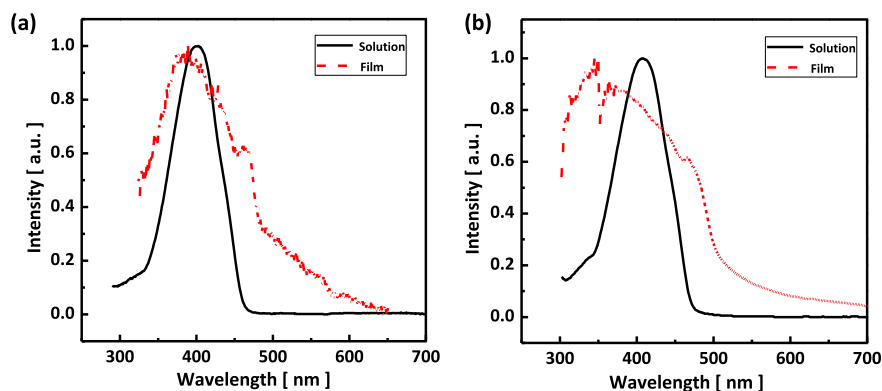


Fig. 2. UV-absorption spectra of CHE3TP (a) and CHE3TN (b).

### 3.3. Crystalline morphology

The charge carrier mobility in an organic transistor is related to the crystallinity of the semiconductor. Out-of-plane XRD studies were performed on the CHE3TP, CHE3TN, and CHE4T films to assess the crystallinities of these films (Fig. 5). The diffraction peaks of the small molecules corresponded to the (100) planes grown up from the semiconductor–dielectric interface. These planes indicated an edge-on orientation. The differences in the interlayer spacings of CHE3TN (29.24 Å,  $2\theta = 3.02^\circ$ ), CHE3TP (25.97 Å,  $2\theta = 3.4^\circ$ ), and CHE4T (22.87 Å,  $2\theta = 3.86^\circ$ ) arose from the molecular lengths of naphthalene, phenylene, and thiophene, respectively. The highly-ordered CHE3TN structure in the out-of-

plane direction and the long-range film uniformity were indicated by the strong intensity and sharpness of the (100) diffraction peak, which correlated with a higher charge carrier mobility than was observed in CHE3TP.

**Table 1**  
Photochemical properties.

	$E_{\text{ox}}^{\text{a}}$ (V)	$\lambda_{\text{max\_solution}}^{\text{b}}$ [nm]	$\lambda_{\text{max\_film}}^{\text{b}}$ film[nm]	$E_{\text{HOMO}}^{\text{a}}$ (eV)	$E_{\text{g}}^{\text{b}}$ (eV)	$E_{\text{LUMO}}^{\text{b}}$ (eV)
CHE3TP	0.97	402	389*, 424, 461	5.43	2.64	2.79
CHE3TN	1.09	408	345*, 364, 465	5.55	2.61	2.94

\* Most strong intensity peak position.

<sup>a</sup> Electrochemical parameter which calculated with CV.

<sup>b</sup> Electrochemical parameter according to the onset of UV absorption.

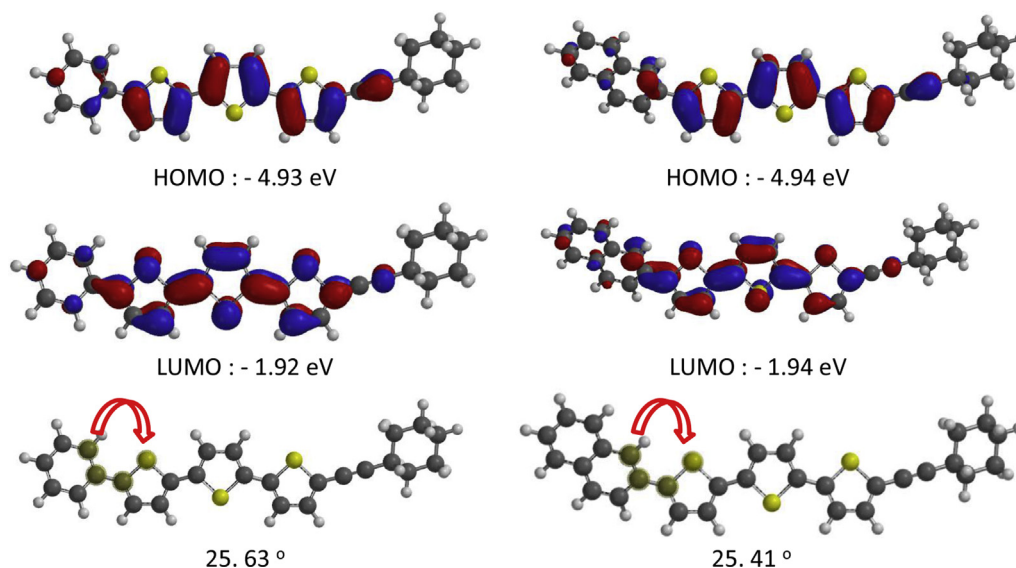


Fig. 3. Molecular orbital surfaces of the HOMOs and LUMOs of the CHE3TP (left) and CHE3TN (right).

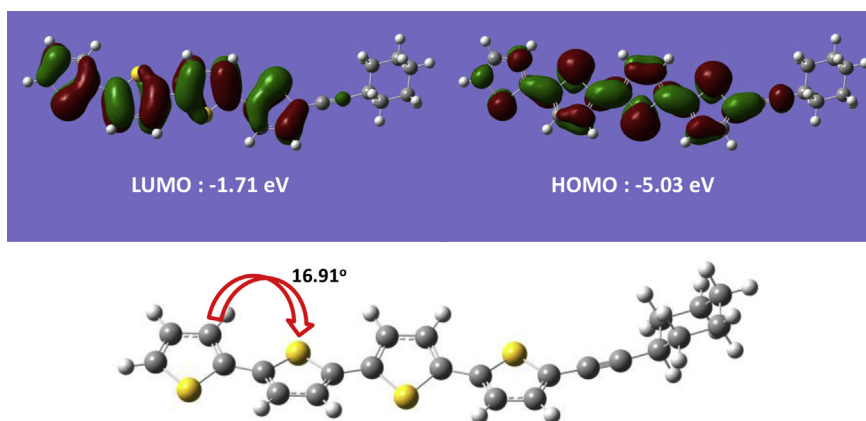


Fig. 4. DFT calculation of CHE4T.

### 3.4. OFET characteristics

The electrical properties of the OFETs prepared using CHE3TP or CHE3TN as semiconductors were characterized, as shown in Fig. 6. The output curves displayed good linear and saturation behavior. The transfer characteristics are summarized in Table 2. The mobility and threshold voltage are average values (7 devices) and other OFET parameters are extracted from plots of Fig. 6 (c) and (d). The higher mobility of CHE3TN compared to CHE3TP arose from the higher solubility of CHE3TN, which formed a highly ordered structure (Fig. 5) and relatively strong intermolecular interactions, corroborated by the UV–vis absorption spectra (Fig. 2) and the DSC measurements (Fig. 1).

Although the phenylene-tri-thiophene and naphthalene-tri-thiophene small molecules showed adequate mobilities for p-type solution processed semiconductors, both mobilities were lower than the mobility of quarter-thiophene (CHE4T, mobility:  $3.21 \times 10^{-2} \text{ cm}^2/\text{V}$ ), reported previously [19]. These results were interpreted as being derived from a trade-off between the phenylene and naphthalene. The tilted phenylene and naphthalene attached to the three-thiophene cores provided better solubility and more homogeneous films compared with the quaterthiophene core (CHE4T); however, the tilted phenylene and naphthalene

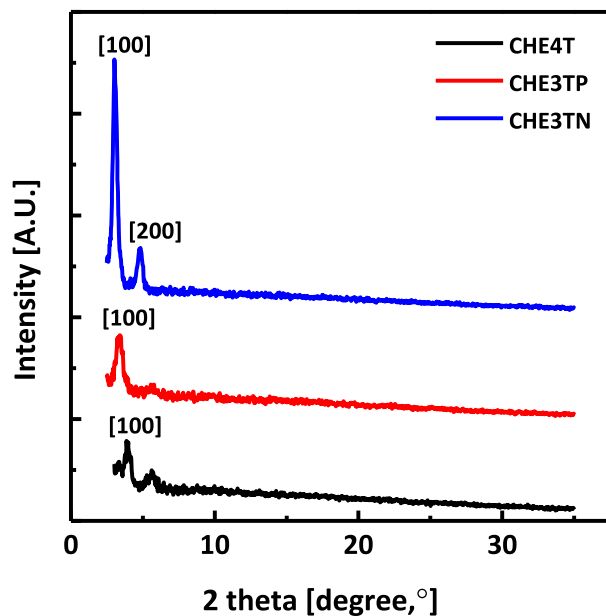


Fig. 5. Out-of-plane direction XRD of CHE4T, CHE3TP, and CHE3TN.

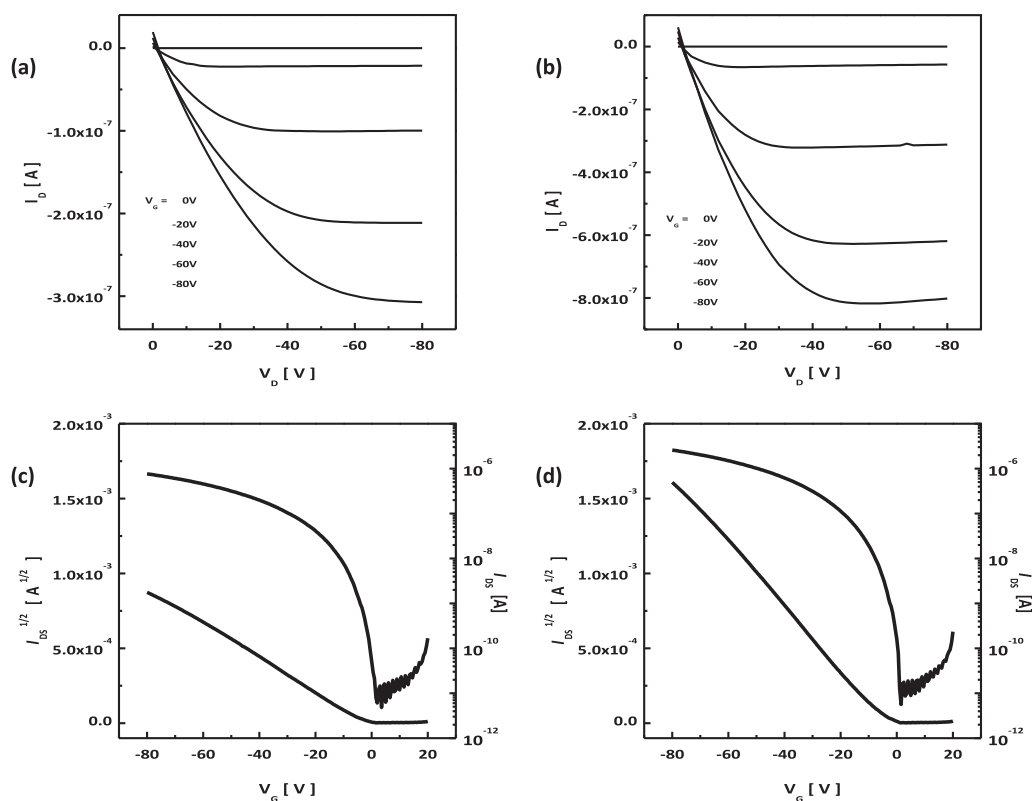


Fig. 6. Output characteristics of thin film transistors based on CHE3TP (a) and CHE3TN (b), Transfer characteristics of CHE3TP (c) and CHE3TN (d).

**Table 2**  
FET properties of CHE3TP and CHE3TN.

	$\mu_{\text{avg}}(\text{cm}^2/\text{Vs})$	On/off ratio	$V_{\text{th,avg}}(\text{V})$	SS
CHE3TP	0.0029	$7.77 \times 10^4$	-2.88	1.17
CHE3TN	0.0104	$4.62 \times 10^5$	-5.50	0.65

disturbed the  $\pi$ -orbital delocalization (Figs. 3 and 4), and thus reduced the charge carrier transfer (Fig. 6).

#### 4. Conclusions

In conclusion, phenylene and naphthalene moieties were combined with a three-thiophene core to form CHE3TP and CHE3TN, respectively. The moieties were tested as replacements for the thiophene in quaterthiophene (CHE4T) in an effort to enhance the solution processability of the small molecules. A greater degree of torsional structure in the CHE3TP and CHE3TN molecules increased the solubility and film uniformity, although this structure also reduced the co-planarity in the conjugated core and mobility. CHE3TN showed the best solubility and crystallinity among the CHE3TP, CHE3TN, and CHE4T molecules tested.

#### Acknowledgments

This study was supported by a grant (2011-0031639) from the Center for Advanced Soft Electronics under the Global Frontier Research Program of the Ministry of Education, Science and Technology. This work was supported by the New & Renewable Energy Technology Development Program of KETEP (20113020010070) and by Nano-Material Technology Development Program of NRF by MSIP (2012M3A7B4049647)

#### References

- [1] Kang I, An TK, Hong J-a, Yun H-J, Kim R, Chung DS, et al. Effect of selenophene in a DPP copolymer incorporating a vinyl group for high-performance organic field-effect transistors. *Adv Mater* 2013;25(4):524–8.
- [2] Yuan Y, Giri G, Ayzner AL, Zoombelt AP, Mannsfeld SCB, Chen J, et al. Ultra-high mobility transparent organic thin film transistors grown by an off-centre spin-coating method. *Nat Commun* 2014;5.
- [3] Katz HE. Recent advances in semiconductor performance and printing processes for organic transistor-based electronics. *Chem Mater* 2004;16(23):4748–56.
- [4] Zhang L, Di C-a, Yu G, Liu Y. Solution processed organic field-effect transistors and their application in printed logic circuits. *J Mater Chem* 2010;20(34):7059–73.
- [5] Brown AR, Jarrett CP, de Leeuw DM, Matters M. Field-effect transistors made from solution-processed organic semiconductors. *Synth Met* 1997;88(1):37–55.
- [6] Payne MM, Parkin SR, Anthony JE, Kuo C-C, Jackson TN. Organic field-effect transistors from solution-deposited functionalized acenes with mobilities as high as  $1 \text{ cm}^2/\text{V}\cdot\text{s}$ . *J Am Chem Soc* 2005;127(14):4986–7.
- [7] Allard S, Forster M, Souharce B, Thiem H, Scherf U. Organic semiconductors for solution-processable field-effect transistors (OFETs). *Angew Chem Int Ed* 2008;47(22):4070–98.
- [8] Gao P, Beckmann D, Tsao HN, Feng X, Enkelmann V, Baumgarten M, et al. Dithieno[2,3-d;2',3'-d']benzo[1,2-b;4,5-b']dithiophene (DTBDT) as semiconductor for high-performance, solution-processed organic field-effect transistors. *Adv Mater* 2009;21(2):213–6.
- [9] Sung Chung D, Kyu An T, Eon Park C, Yun H-J, Kwon S-K, Kim Y-H. High-speed solution-processed organic single crystal transistors using a novel triisopropylsilyl ethynyl anthracene derivative. *Appl Phys Lett* 2012;101(19):193304.
- [10] An TK, Jang SH, Kim S-O, Jang J, Hwang J, Cha H, et al. Synthesis and transistor properties of asymmetric oligothiophenes: relationship between molecular structure and device performance. *Chem Eur J* 2013;19(42):14052–60.
- [11] An TK, Park S-M, Nam S, Hwang J, Yoo S-J, Lee M-J, et al. Thin film morphology control via a mixed solvent system for high-performance organic thin film transistors. *Sci Adv Mater* 2013;5(9):1323–7.
- [12] Zhang J, Wu G, He C, Deng D, Li Y. Triphenylamine-containing D-A-D molecules with (dicyanomethylene)pyran as an acceptor unit for bulk-heterojunction organic solar cells. *J Mater Chem* 2011;21(11):3768–74.
- [13] Minemawari H, Yamada T, Matsui H, Tsutsumi Jy, Haas S, Chiba R, et al. Inkjet printing of single-crystal films. *Nature* 2011;475(7356):364–7.

- [14] Kim DH, Park YD, Jang Y, Yang H, Kim YH, Han JI, et al. Enhancement of field-effect mobility due to surface-mediated molecular ordering in regioregular polythiophene thin film transistors. *Adv Funct Mater* 2005;15(1):77–82.
- [15] Atkins P, De Paula J. *Physical chemistry*. Oxford University Press; 2006.
- [16] Guo X, Ortiz RP, Zheng Y, Kim M-G, Zhang S, Hu Y, et al. Thieno[3,4-c]pyrrole-4,6-dione-Based polymer semiconductors: toward high-performance, air-stable organic thin-film transistors. *J Am Chem Soc* 2011;133(34):13685–97.
- [17] Wang L, Nan G, Yang X, Peng Q, Li Q, Shuai Z. Computational methods for design of organic materials with high charge mobility. *Chem Soc Rev* 2010;39(2):423–34.
- [18] Mei J, Diao Y, Appleton AL, Fang L, Bao Z. Integrated materials design of organic semiconductors for field-effect transistors. *J Am Chem Soc* 2013;135(18):6724–46.
- [19] An TK, Hahn S-H, Nam S, Cha H, Rho Y, Chung DS, et al. Molecular aggregation–performance relationship in the design of novel cyclohexylethynyl end-capped quaterthiophenes for solution-processed organic transistors. *Dyes Pigments* 2013;96(3):756–62.
- [20] Kim S-o, An TK, Chen J, Kang I, Kang SH, Chung DS, et al. H-Aggregation strategy in the design of molecular semiconductors for highly reliable organic thin film transistors. *Adv Funct Mater* 2011;21(9):1616–23.
- [21] Zhigalko MV, Shishkin OV, Gorb L, Leszczynski J. Out-of-plane deformability of aromatic systems in naphthalene, anthracene and phenanthrene. *J Mol Struct* 2004;693(1–3):153–9.
- [22] Paolo S, Irakli S, Viola F, Klaus M, Jürgen PR. Nanoribbons from conjugated macromolecules on amorphous substrates observed by SFM and TEM. *Nanotechnology* 1999;10(1):77.
- [23] Lee MW, Cha SB, Yang SJ, Park SW, Kim K, Park NG, et al. Synthesis of organic dyes with linkers between 9,9-dimethylfluorenyl terminal and a-cyanoacrylic acid anchor, effect of the linkers on UV–vis absorption spectra, and photo-voltaic properties in dye-sensitized solar cells. *Bull Korean Chem Soc* 2009;30(10):2269–79.
- [24] Klauk H. Organic thin-film transistors. *Chem Soc Rev* 2010;39(7):2643–66.
- [25] Hwang MC, Jang J-W, An TK, Park CE, Kim Y-H, Kwon S-K. Synthesis and characterization of new thermally stable poly(naphthodithiophene) derivatives and applications for high-performance organic thin film transistors. *Macromolecules* 2012;45(11):4520–8.
- [26] Facchetti A, Letizia J, Yoon M-H, Mushrush M, Katz HE, Marks TJ. Synthesis and characterization of diperfluorooctyl-substituted phenylene–thiophene oligomers as n-type semiconductors. Molecular structure–film micro-structure–mobility relationships, organic field-effect transistors, and transistor nonvolatile memory elements. *Chem Mater* 2004;16(23):4715–27.
- [27] Cowie JMG. Polymer characterization–chain dimensions, structures, and morphology. In: Arrighi V, editor. *Polymers: chemistry and physics of modern materials*. 3 ed. Boca Raton: CRC Press; 2008. pp. 253–77.
- [28] Cowie JMG. The crystalline state and partially ordered structures. In: Arrighi V, editor. *Polymers: chemistry and physics of modern materials*. 3 ed. Boca Raton: CRC Press; 2008. pp. 279–319.